One-step strategy of 3D hierarchical porous carbon with self-heteroatom-doped derived bread waste for high-performance supercapacitor

by Rika Taslim

Submission date: 12-Apr-2023 01:37PM (UTC+0700)
Submission ID: 2062334343
File name: 2._JAAP_2023.pdf (3.3M)
Word count: 10135
Character count: 55541

Journal of Analytical and Applied Pyrolysis 171 (2023) 105956

Contents lists available at ScienceDirect

Journal of Analytical and Applied Pyrolysis

journal homepage: www.elsevier.com/locate/jaap

One-step strategy of 3D hierarchical porous carbon with self-heteroatom-doped derived bread waste for high-performance supercapacitor

Rika Taslim [a], Refky Refanza [a], Muhammad Ihsan Hamdy [a], Apriwandi Apriwandi [b], Erman Taer [b]

[a] Department of Industrial Engineering, Faculty of Science and Technology, State Islamic University of Sultan Syarif Kasim, Riau 28293, Indonesia
[b] Department of Physics, Faculty of Mathematics and Natural Sciences, University of Riau, Riau 28293, Indonesia

ARTICLE INFO

Keywords:
d waste
Hierarchical porous carbon
Electrode materials
Supercapacitor

ABSTRACT

Bio-waste is a promising carbon source that can be used as a basic component in renewable supercapacitors due to its abundant hierarchical pore structure potential, heteroatom self-doping capability, high surface area, as well as well-defined chemical and mechanical stability. This study converted bread bio-waste into rich 3D hierarchical porous carbon through a one-step facile strategy to be used as the main component of a supercapacitor. The porous carbon was obtained through physical activation approach at different temperatures of 750, 800, 850, and 900 °C without being combined with chemical activation. The optimized activated carbon illustrated high porosity behavior with an abundant 3D hierarchical pore structure consisting of 76.98% micropores and 23.02% mesopores and also produced a well-defined wettability of self-d g heteroatoms. Moreover, the electrochemical behavior in a symmetric supercapacitor cell showed a high specific capacitance of 202 F g^{-1} at 1 A g^{-1} with a rate capability of 73% 0 mV s^{-1} in a 1 M H_2SO_4 electrolyte. It was also discovered that the activation temper e of 850 produced the highest energy density of 11.61 Wh kg^{-1} at a power density of 156. W kg^{-1} with a low equivalent series resistance of 0.11 Ω. Finally, the proof-of-concept showed that bread waste has immense potential as a 3D hierarchical porous carbon source after the synthesis through a single-stage facile approach and can be used as a major renewable electrode component for sustainable supercapacitors.

1. Introduction

Waste is one of the major global problems as indicated by the production of at least 2.12 billion tons of waste consisting of solid, industrial, organic, inorganic-chemical, liquid, agricultural-forest-land, and food wastes on a large scale [1]. The increasing industrialization, the current economic situation which is on the verge of a 2023 recession, and riots leading to wars between different countries are projected to increase this figure to 3.40 billion tons by the end of 2050 [2]. The drastic increase simultaneously has a negative impact on the survival of mankind, especially due to the application of coordinated open and direct burning as the management method for at least 33% of the total waste [3]. This conventional treatment affects air-water quality, public health, and the environment. Food waste was found to be one of the largest contributors to the total volume of waste due to uncontrolled population growth. It is considered to have the ability of crippling a country's economy [4] because so much wastewater is used for agriculture, labor, and electricity that is lost in the food processing industry and even contributes to deforestation considering all the true value for money per year [5]. This has led researchers, academics, practitioners, and world governments to work together by providing their thoughts on the efforts to reduce the accumulation of waste using methods without negative impacts. Materials science studies suggest a zero-waste approach through the reuse and modification of basic materials from waste. Some of these studies reconstructed plastic waste into a second product while others treat solid-liquid waste to increase soil fertility and planting media in agriculture and plantation aspects [6,7]. In a wider application, wastes also have the potential to be used as an energy source in the form of biofuel, bioethanol, and others [8,9].

It was interestingly stated that the main element of most of these s tes including urban solid, agricultural, and food wastes is carbon which can be utilized in different high-level applications such as water

* Corresponding author.
E-mail address: rikataslim@gmail.com (R. Taslim).

https://doi.org/10.1016/j.jaap.2023.105956
Received 28 November 2022; Received in revised form 14 March 2023; Accepted 15 March 2023
Available online 16 M ch 2023

purification, heavy metal sequestration, renewable energy systems, and energy storage devices [10–13]. The physicochemical characteristics of bio-waste-based carbons such as well-defined pore framework, high surface area, manageable hierarchical pore distribution, as well as good thermal and chemical stability enable their application in energy storage devices and outstanding performance enhancement in the classification of supercapaci [14–16]. Previous studies have shown that these supercapacitor electrochemical energy storage devices have excellent power density and increased energy density compared to conventional batteries and capacitors [17,18]. Moreover, their life cycle is unlimited (in theory) with great stability and this confirms their high potential in sustainable technologies [19,20].

Several studies have reported different approaches and strategies to convert biowaste into carbon, especially porous activated carbon for supercapacitor device components. From the beginning of 2012 to the end of 2015, porous carbons were synthesized through chemical activation, carbonization, physical activation, and hydrothermal approaches [21–23] with mostly agricultural and agro-industrial biomass sources such as bamboo [24], willow catkins [25], date palm trees [22], and rotten potatoes [26] for supercapacitor application. These methods have significantly demonstrated that high-fix carbon with a specific surface area favors high electrochemical performance. Moreover, the reported techniques are markedly superior in terms of high surface area, low cost, time-saving, free of corrosive and toxic, and environmental friendliness. However, the electrochemical behavior was observed to have a low energy density and relatively inconsistent with its high-power density. In the last four years, researchers have suggested that energy density can be increased by modifying the pore structure of carbonaceous materials which are required to have appropriate pore combinations with hierarchically connected structures [27,28]. Furthermore, the combination of micro, meso, and macropores confirmed on activated carbon simultaneously has abundant active sites for ions to form an electrical double layer, a short transport path, and very fast ion accessibility with 3D movement in all directions [27,29]. Jiang et al., 2020 converted peanut shells into activated carbon with 3D hierarchical pore structures by adding a dopant through chemical activation–carbonization combination approach [30] and were able to increase the energy density up to 4 times compared to previous report. Similar results have also been confirmed by Selvaraj et al., 2021 through the production of 3D hierarchical porous carbon from *Prosopis juliflora* wood for a supercapacitor device at an energy density of 32.9 W h kg^{-1} [31]. However, the preferred approach of combining several strategies to produce carbon synthesis which is relatively time-consuming and costly hampers renewability. It was also discovered that not all bio-wastes showed the potential of a 3D hierarchical pore framework despite being treated with these techniques. Therefore, it is necessary to study an easy, one-step, and cost-effective strategy as well as a credible source of materials to obtain 3D hierarchical porous activated carbon for sustainable electrochemical energy storage devices.

Bread waste is considered a very serious problem in big countries, especially developed ones. This is observed in the domination of the global annual bread production of more than 100 million tons by the European market at 53.6%, the United States at 28.6%, the Asia Pacific at 10.9%, and the Middle East and African countries at 6.9% [32]. It has been estimated that 10% of all bread produced is wasted and its organic biogenic nature shows its ability to pose serious risks to the public and environmental health and also pollute natural habitats [33]. Meanwhile, bread ingredients categorized as organic have been converted as a carbon source for supercapacitor applications. Several previous studies have prepared bread waste-based carbon through the N_2 reactor pyrolysis approach with the addition of metal oxide doping techniques [32,34]. The porous carbon obtained showed the characteristics of 88% carbon with a confirmed micro-mesoporosity structure. However, their electrochemical properties are very low 40–87 F g^{-1} [34]. In addition, the strategy of metal oxides doped is considered to limit the sustainable application due to metal residues and corrosiveness.

This study was used to synthesize 3D hierarchical porous activated carbon from bakery waste produced through a one-step approach as the main electrode component for continuous supercapacitor applications. Bread waste was converted into activated carbon through a one-stage physical activation technique without involving chemical activation, carbonization, and hydrothermal in order to save time, cost, and energy. Furthermore, the electrochemical properties were measured in the solid design without adding a binder such as PVA, PTFE, or PFDV. The results obtained showed the real performance of the supercapacitor device while the activated carbon illustrated an abundant 3D hierarchical pore structure with increased wettability through heteroatom functional groups. Moreover, the electrochemical behavior obtained showed a high specific capacitance of 202 F g^{-1} with an increased energy density of 11.61 Wh kg^{-1}. This study finally proved the potential of bread waste as a 3D hierarchical porous activated carbon produced through a one-step approach in high-performance supercapacitors application.

2. Materials and methods

2.1. Materials

The study used 1000gr of bread waste collected from existing bakery outlets in Pekanbaru, Indonesia, and also ensure all chemicals are of analytical grade. Moreover, the KOH chemical reagent used was from Merck KGaA, EMD Milliore Corporation with code No. B1890433 108 while 98% purity H_2SO_4 chemical reagent was provided from panreac qiumica sau, espana, code No. 131058, 1612. The organic membrane used as a separator was obtained from duck eggshells and DI water produced on a laboratory scale.

2.2. Bread waste-based porous carbon preparation

Bread wastes were cut into small pieces of 1×2cm size and dried in a low-temperature oven of 110 °C for 36 h. The mass loss of the sample was reviewed periodically for 12 h until the reduction was constant. The dried precursors were pre-carbonized in a vacuum oven at a maximum temperature of 250 °C for 2 h and 30 min after which the brittle products were crushed and ground in a milling machine into a powdered precursor [35]. The powder was filtered using a 250-mesh sieve to obtain a powder precursor with size < 60 μm and this was followed by the application of the method frequently used in previous studies and considered to be easy and time-saving [36]. This study designed solid precursors at the start of treatment to maintain real conductivity properties [37] and they were obtained without the addition of binder by pressing the precursor powder in a pressing machine at a pressure equivalent to 8 tons. Moreover, thin coin-shaped solid precursors at certain dimensions were pyrolyzed at high temperatures in the gaseous environment of N_2 and CO_2 alternately. The pyrolysis temperature set on a scale of 600 in the N_2 gas environment and 750, 800, 850, and 900 °C in the CO_2 gas environment. This led to the production of activated solid carbon which was subsequently neutralized in DI water immersion. Therefore, the activated solid carbons produced were labeled 750_{HPC}BW, 800_{HPC}BW, 850_{HPC}BW, and 900_{HPC}BW based on different pyrolysis temperature parameters.

2.3. Material characterization

The solid precursors were initially evaluated in terms of their dimensions including mass, thickness, and diameter against the effect of high-temperature pyrolysis expressed explicitly in density through standard equations. The mass was measured using an electric balance with 0.0001 gr precision, thickness, and diameter through a caliper with 0.001 mm uncertainty, and density was calculated using the equation $\rho = m/V$ [38]. Furthermore, the microcrystalline properties and phase changes of porous carbon were reviewed using the x-ray diffraction (XRD) technique on the XPERT-PRO-PW3050/60 Diffractometer system

instrument with anode material Cu $K\alpha_1$ = 1.54060 Å. The XRD parameters were also evaluated based on Braggs law and the Debyee-Shereer equation [39] while scanning electron microscopy (SEM) was used to examine the morphological structure of the ZEISS-EVO10 instrument. Moreover, the porosity was recorded via nitrogen adsorption/desorption isotherms using a Quantachrome TouchWin v1.22 instrument analyzer at a liquid nitrogen temperature of 77 K. The specific surface area was also calculated using the BET (Brunauer–Emmett–Teller) approach, the micropores surface area was measured using the t-plot method, and the pore size distribution was evaluated using the BJH (Barrett-Joyner-Halenda) method.

2.4. Electrochemical performance measurement

The electrochemical properties were evaluated in a symmetrical supercapacitor system designed to resemble two stacks of bond-free solid electrodes with a diameter of 9 mm and thickness of 0.2 mm. The working electrode was also prepared in a 1 M H_2SO_4 acid electrolyte solution separated by an organic separator based on a duck eggshell membrane [40] with a thickness of 0.1 mm. Moreover, the electrochemical behavior was measured using a cyclic voltammetry technique with the CVUR-RADER5841 instrument ± 6.05% ERROR CALIBRATED VersaStat II Princeton Applied Research at a potential of 0–1 V at 1–10 mV s^{-1}. The capacitive properties (C_{sp}, F g^{-1}), energy density (E_{sp}, Wh kg^{-1}), and power density (P_{sp}, W kg^{-1}) were evaluated in a complex manner through a galvanostatic charge-discharge method at 1–10 A g^{-1} using CDUR-RADER2018 ± 6.00% ERROR CALIBRATED VersaStat II Princeton Applied Research Furthermore, the interaction of the carbon electrode with the selected aqueous electrolyte was confirmed through electrochemical impedance spectroscopy (EIS) analysis performed in the frequency range of 0.01 Hz–100 kHz in an open circuit with 10 mV amplitude. The electrochemical parameters were further calculated in detail through the following equations:

$$C_{sp} = \frac{I \bullet \Delta t}{m \bullet \Delta V} \quad (1)$$

$$E_{sp} = \frac{C_{sp} \bullet \Delta V^2}{7.2} \quad (2)$$

$$P_{sp} = \frac{3600 \bullet E_{sp}}{\Delta t} \quad (3)$$

where, I is the current (A), m is the mass of the working electrode (g), Δt is the charge-discharge time (s), and ΔV is the working potential (V).

3. Results and discussion

The high temperature used in the pyrolysis of solid precursors simultaneously affects their dimensions and those consisting of a carbonization process in inert gas N_2 and physical activation in a CO_2 gas environment usually allows the decomposition of organic-inorganic compounds in bread waste, thereby, reducing the density of precursors. It was discovered that the density of the solid precursors before pyrolysis in gaseous N_2 and CO_2 environments ranged from 0.8721 to 0.8424 g cm^{-3} with a measurement error of ± 0.01 for each x_{HPC}BW sample. Bread is generally produced from a specific composition that always contains carbohydrates, fats, proteins, and small amounts of calcium, phosphorus, and iron. This composition undergoes degradation and evaporation during the pyrolysis process. As is commonly known, carbonization from 30 °C to 600 °C in an inert gas plays an important role in evaporating the volatile, lignocellulosic, carbohydrate, and fat compounds, followed by the inorganic components of the bio-raw material [41]. Exhaust steam is channeled in the form of H_2O, CO, and CO_2 [42]. However, this process leaves tar residue, thus further treatment is needed. The integrated one-stage physical activation process at different maximum temperatures (750, 800, 850 and 900 °C) enables tar removal, optimum pore framework growth, and maximizes carbon porosity potential [43]. Therefore, the combination of the integrated carbonization and physical activation processes was discovered to have significantly reduced the densities of the samples by 0.6234, 0.6329, 0.5254, and 0.5003 g cm^{-3} for the precursors of 750_{HPC}BW, 800_{HPC}BW, 850_{HPC}BW, and 900_{HPC}BW, respectively. It was discovered that the physical activation at 750 °C had the smallest solid precursor density reduction of 12.06% while the addition up to 800, 850, and 900 °C degraded the higher density from 13.4% to 32.27%. This suggests that an increased physical activation allowed the enhanced carbon frameworks to produce abundant pore structures. These features are urgently needed to provide a high specific surface area for the ionic charge and a relatively fast electrolyte transfer path [44]. Moreover, there is a need for more detailed confirmation on the effect of physical activation on the pore structure of carbon with a focus on the precursors of 750_{HPC}BW and 850_{HPC}BW because the density reduction was lowest and highest at 750 °C and 850 °C respectively (Fig. 1).

The morphological and microstructure modifications of the precursor carbon in different treatments were reviewed using SEM measurements and the results are presented in Fig. 2. It was discovered that a clear weight loss occurred as confirmed by density analysis when the precursor material was pyrolyzed at high temperatures under a nitrogen and carbon dioxide atmosphere due to the decomposition of organic, inorganic, and complex compounds of carbohydrates, fats, proteins, and some ash and tar. During the decomposition process, the bonds of carbohydrates and fats were broken down simultaneously followed by degradation of their content which was mostly released in the form of gases including CO_2, N_2, H_2O, and others. This means the precursor of bread waste was significantly converted into highly pure carbon with a defined micromorphological structure.

Fig. 2a-e show that the physical activation temperature in the CO_2 gas environment has a significant impact on the growth of the pore morphological structure of the precursor which the SEM image of the 750_{HPC}BW in Fig. 2a shows an uneven morphology. For the most part, the surface morphology has chunks of particles and carbon blocks dotted with flakes but pore skeletons have been formed as shown in Fig. 2b. In the selected magnification area, 750_{HPC}BW was discovered to have the potential for the formation of hierarchical combination pores characterized by a structure resembling random bubbles which is similar to sponge morphology. The pores were observed to look random and shallow and this confirmed that the 750_{HPC}BW retains the original shape of the bread and this is believed to have the ability of improving the performance of the electrode in terms of accessibility and fast charge transfer [45]. The physical activation of CO_2 at 750 °C significantly reduced the lignocellulosic component and initiated the formation of a pore framework in the precursor but this temperature is too low for the activation process to maximize the growth of 3D hierarchical pores.

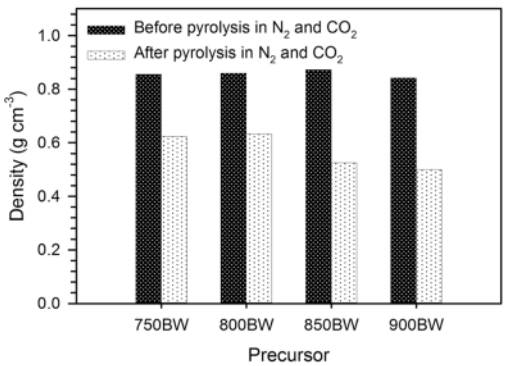

Fig. 1. The density of the solid precursors before and after pyrolysis in gaseous N_2 and CO_2 environments.

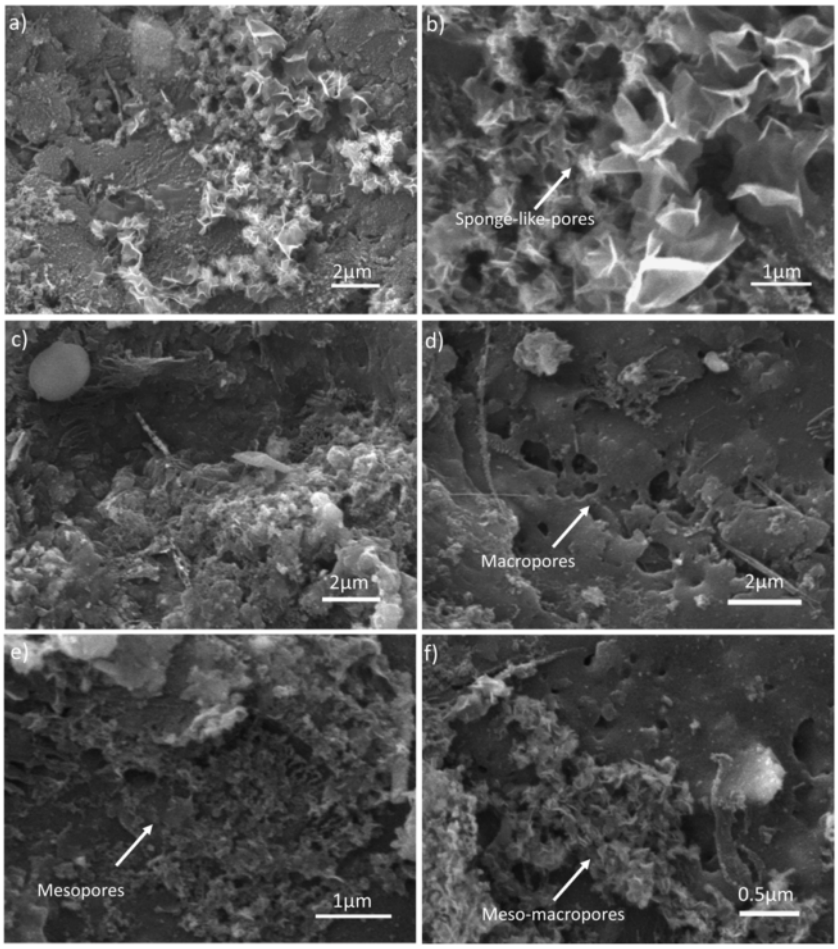

Fig. 2. The image SEM of (a-b) 750_{HPC}BW and (c-f) 850_{HPC}BW.

Fig. 2c shows the pore morphology of 850_{HPC}BW which markedly presents abundant pores of different sizes and this is significantly different from the precursor 750_{HPC}BW. This confirms that 850 °C has a high potential for the preparation of porous carbon-based biomass. Furthermore, the selected area in Fig. 2d showed that 850_{HPC}BW exhibits a deep and large maze-well-like pore structure with a size of 348–1265 nm which is classified as macroporous. This means it can act as an ion buffer in the electrode material to provide access for ion diffusion in all directions [46], thereby, ensuring the supercapacitor devices have extraordinary power density. It was further discovered in Fig. 2e that the 850_{HPC}BW has an abundant mesoporous structure covering all precursor surfaces with pore sizes in the measuring range of 34–49 nm. These high mesopores are very beneficial to achieving fast ion accessibility and low internal resistance which are needed to maintain the real conductivity of the original material [47]. Interestingly, the 850_{HPC}BW also indicates a micropores structure on its surface characterized by abundant small white spots as presented in Fig. 2f and this allows the carbon material to have abundant electrically charged contact sites corresponding to the size of the selected electrolyte ion [48]. All the aforementioned results showed that 850_{HPC}BW has a 3D hierarchical pore structure consisting of a combination of macropores, mesopores, and micropores. These features work together to boost electrode performance, thereby, allowing the energy storage devices to have an increased energy density and maintain a high power density [49].

The changes in the microstructure and phase shift of the carbon obtained were reviewed through electron diffraction patterns in the selected area. It was, therefore, discovered from Fig. 3 that the X-ray diffraction patterns of 750_{HPC}BW and 850_{HPC}BW adopted amorphous features and high crystalline degradation of carbon walls as evidenced

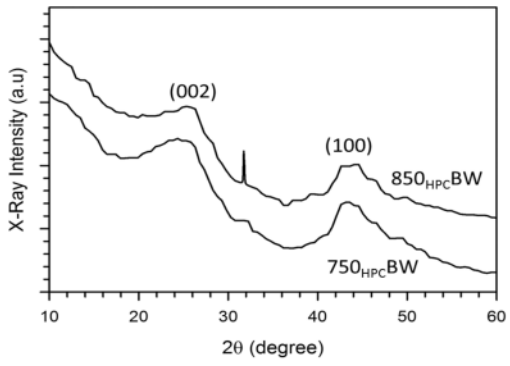

Fig. 3. XRD pattern of 750_{HPC}BW and 850_{HPC}BW.

by wide bumps at 24° which correlate with scattering (002) [50]. Furthermore, the broad-weak peak estimated at 44° which is identical to the scattering plane (100) indicates a reduction in the graphite carbon lattice to produce a turbostratic-disturbed carbon structure [51,52]. This distinctive XRD pattern demonstrates the pore-rich carbon structure along the surfaces at different si[49] [53]. The higher intensity observed at the low 2θ angle area can also be ascribed to the presence of abundant micropores in the x_{HPC}BW and this was also clearly confirmed in the SEM images presented in Fig. 2. The deeper and higher heat treatment was discovered to have allowed a decrease in the intensity of the weaker peak width, thereby, indicating the development of high carbon lattice damage which initiated the formation of a 3D-connected hierarchical pore framework [54]. This assumption was confirmed more deep[6] through the analysis of the N_2 adsorption-desorption isotherm. In addition, the XRD pattern also revealed low sharp peaks at an angle of 31° confirming the presence of oxide compounds of $CaCO_3$ (JCPDS No. 82–1690) donated from common compounds of biomass [37,55]. In general, Ca elemental acts as an inhibitor of ion di[21]on. Interestingly, the oxygen element attached to the carbon chain is closely related to the increase in the material's wettability, due to a self-doping effect in the electrode material. A similar analysis was also revealed in previous studies [54,56]. Furthermore, the detailed summary presented in Table 1 showed that the prepared carbon had low graphitization due to its porous structure which is evident in the larger interlayer spacing $d_{(002)}$ of 0.3631–0.3647 nm which is approximately 9.34% higher than 0.33354 nm recorded for $d_{(002)}$ graphite [57]. It was also observed that the interlayer spacing in the scattering plane $d_{(100)}$ possesses a relatively constant value at 0.204 nm which characterizes the st[19]re of activated carbon produced from organic wastes. Moreover, the increase in the physical activation temperature from 750 °C to 850 °C led to a degraded L_c lattice height value and an increased L_a lattice width value. This is considered to be their contribution towards improving the porosity properties of the porous carbon prepared[44]e carbon lattice height (L_c) in the XRD pattern analysis is often associated with the prediction of the specific surface area of the carbon obtained with several previous studies observed to have provided an inverse relationship between L_c and surface area through certain reported empirical equations [58,59]. Some reviews also indicated that a higher temperature at 850_{HPC}BW is predicted to have better porosity properties with a higher specific surface area and this was confirmed more deeply through the N_2 isotherm adsorption-desorption ana[42].

The features of porosity, pore structure, and pore size distribution of the x_{HPC}BW carbon obtained were characterized by nitrogen phys[36]ption and analysis based on BET, T-plot, and BJH approaches. Fig. 4 shows the adsorption-desorption isotherm of N_2 and the pore size distribution of the bread waste-based activated carbon including 750_{HPC}BW and 850_{HPC}BW. The precursor 750_{HPC}BW was observed to have displayed a typical imperfect type IV isotherm profile with a high first absorption point at relatively low pressures and this characterizes an abundant micropores structure and growing mesopor[5] [60,61]. However, this type of isotherm is relatively awkward with a long and open hysteresis loop along a relative pressure of p/p_0 ranging fro[34]01 to 1.00. This proves that 750_{HPC}BW has poor porosity behavior with a specific surfa[64]ea of 196,899 $m^2\ g^{-1}$ and micropores of about 69.41% at a narrow average pore diameter of 1.23919 nm. In addition, the discrepancy in the open hysteresis loop is a strong indication of a rudimentary mesoporous material with a cylindrical structure, a narrow pore neck, and a wide interior [62]. This form simultaneously inhibits desorption of N_2 gas and displays the characteristics of an imperfect hysteresis loop. Meanwhile, the increment of the activation temperature up to 850 °C showed a significantly different isothe[65] curve. The 850_{HPC}BW isotherm curve generally confirms the ty[29]l combination of type I and IV with high adsorption at low relative pressure $p/p_0 \leq 0.1$ and complete hysteresis loop at higher relative pressure $0.41 \leq p/p_0 \leq 0.93$ and this proves that the samples have rich micropores and mesopores [63]. In more detail, the precursor 850_{HPC}BW showed high porosity wi[33]e specific surface area increased almost fourfold as high as 610.507 $m^2\ g^{-1}$ at a higher total volume of 0.391071 $cm^3\ g^{-1}$. The higher absorption at the starting point confirmed the rapid micropores growth reaching 469.986 $m^2\ g^{-1}$ which at least dominated 76.98% of the total surface area of the 850_{HPC}BW. This feature significantly contributes to the provis[47] of highly active sites for the electrolyte anions to form an abundant electrical double layer at the electrode/electrolyte interface [64]. However, the hysteresis loop type H2 showed good mesoporous with a narrow porous cylindrical structure in the range of 3.1–28.2 nm and the area reached 140.521 $m^2\ g^{-1}$ with 38.25% of the total volume of 850_{HPC}BW. A more detailed range of mesoporous sizes obtained from the prepared carbon is shown in Fig. 4b and this well-defined mesoporous behavior is required by electrode materials to provide short access paths and fast ion transport in energy storage devices [65]. It was comprehensively discovered that 850_{HPC}BW confirmed their porosity potential which involves hierarchically-linked micropores and mesopores, thereby, enabling the enhancement of their electrochemical properties in supercapacitor devices [66]. The complete porosity properties of 750_{HPC}BW and 850_{HPC}BW are summarized in detail in Table 2 while those related to 800_{HPC}BW and 900_{HPC}BW precursors are not presented in this study due to their short pyrolysis temperature range. It was indicated in the table that 750_{HPC}BW and 850_{HPC}BW did not have any significant effect on porosity but the pore volume increased slightly with increasing temperature due to increased degradation of C species. It is important to note that this analysis was based on a previous work that provided a similar treatment for organic waste-based carbon sources.

[2] This study used three complete combination approaches including cyclic voltammetry (CV), galvanostatic charge-discharge (GCD), and electrochemical [59]edance spectroscopy (EIS) in a two-electrode sandwich system to evaluate the electrochemical efficiency of the hierarchical porous carbon produced from breadcrumbs using a very easy approach without chemical injection. The dominant electrochemical behavior of x_{HPC}BW was confirmed using cyclic voltammetry from 0 to 1.0 V voltage in a graded scan from 1 to 5 mV s^{-1} and the CV measurement curves of 750_{HPC}BW, 800_{HPC}BW, 850_{HPC}BW, and 900_{HPC}BW at 1 mV s^{-1} are presented in Fig. 5a. It was generally observed that the electrochemical behavior led to well-defined types of electrical double-layer capacitors (EDLCs) [67]. In addition, the relative growth of "camel-humps" was reflected in their hysteresis loop which was characterized by a marked increase in current density over a potential range of 0.35–0.82 V. This feature is closely related to functional groups of heteroatoms that produced an independent doping effect on the electrode material [68,69]. Moreover, the elements of oxygen and nitrogen were strongly indicated as self-doping in the x_{HPC}BW material which subsequently added to the pseudo-ca[3]itance behavior in supercapacitor devices. It is interesting to note that the increase in the heating temperature from 750 °C to 850 °C drastically amplified this feature and this confirms the production of self-doping oxygen in the broken carbon chain [70]. This critically influenced the addition of their capacitive properties. However, an increase to a higher temperature of 900 °C significantly reduced their pseudo-capacitance due to evaporation and excessive erosion of the carbon chain. On the plus side, the ideal EDLCs were featured among other materials. Furthermore, the capacitive properties of the material can also be confirmed by the magnitude of the resulting hysteresis loop and the standard equation applied showed that the specific capacitances of 750_{HPC}BW, 800_{HPCB}W, 850_{HPC}BW, and 900_{HPC}BW were 135, 189, 199, and 110 F g^{-1}, respectively. This means

Table 1
XRD parameter[3] 750_{HPC}BW and 850_{HPC}BW.

Precursor	$2\theta_{(002)}$ (°)	$2\theta_{(100)}$ (°)	$d_{(002)}$ (nm)	$d_{(100)}$ (nm)	L_c (nm)	L_a (nm)
750_{HPC}BW	24.49	44.26	0.36	0.21	1.07	3.40
850_{HPC}BW	24.38	44.14	0.26	0.22	0.86	4.50

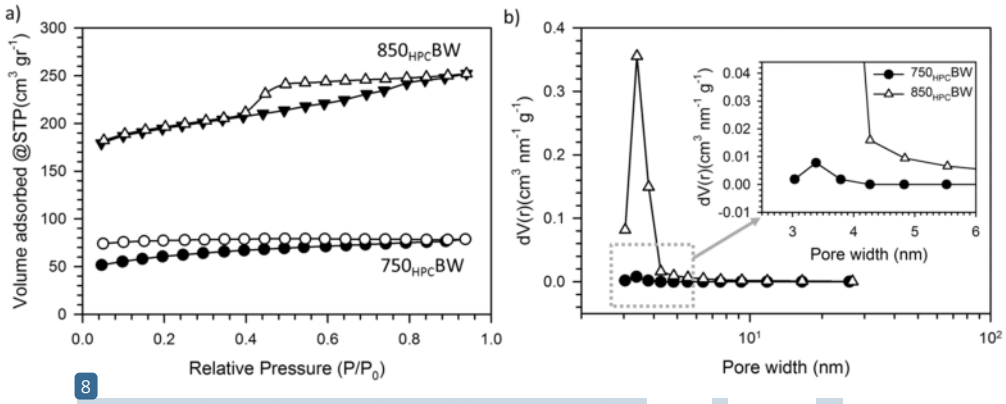

Fig. 4. (a) N_2 adsorption-desorption isotherms and (b) pore size distribution profiles of $750_{HPC}BW$ and $850_{HPC}BW$.

Table 2
Porosity properties of 750HPCBW and 850HPCBW.

Precursor	S_{BET} (m^2 g^{-1})	S_{mic} (m^2 g^{-1})	S_{meso} (m^2 g^{-1})	V_{tot} (cm^3 g^{-1})	V_{mic} (cm^3 g^{-1})	V_{meso} (cm^3 g^{-1})	D_{av} (nm)
$750_{HPC}BW$	196.9	136.7	60.2	0.122	0.069	0.053	1.2
$850_{HPC}BW$	610.5	470.0	140.5	0.391	0.242	0.149	1.3

a dramatic increase in the heat treatment produced high capacitive properties as indicated by the increase in the specific capacitance from $750_{HPC}BW$ to $850_{HPC}BW$ by 47.75% at a scan rate of 1 mV s^{-1}. This is associated with the occurrence of optimal etching of the carbon chains on their walls at high temperatures especially 850 °C which led to the production of a well-matched pore framework (confirmed in SEM image) and high specific surface area (610.50 m^2 g^{-1}) with ionic charge transfer and excellent accessibility at the electrode/electrolyte interface material [71]. On the positive side, the self-doping of the heteroatoms contributed to the pseudo-capacitance and this adds to their high capacitive feature. Meanwhile, the treatment at higher heat produced contrasting results with the $900_{HPC}BW$ observed to have shown the smallest capacitive properties compared to the others due to the removal of too much carbon chain which led to the drastic reduction in the accessibility of ions. The EDLC dominant behavior of $x_{HPC}BW$ was also reviewed at higher scan rates and the results presented in Fig. 5b-d generally showed that all the materials retain their distorted rectangular shape, thereby, characterizing the properties of normal double-layer capacitors at a scan rate of 5 mV s^{-1}. This proves that the hierarchical porous carbon material produced from bread wastes has good accessibility to function in electrochemical energy storage devices [72]. The pseudo-capacitance effect was also observed to gradually disappear as the scanning rate increased and this simultaneously led to the reduction of capacitive properties of the original material. This was indicated in the specific capacitance of $x_{HPC}BW$ at different scan rates presented in Fig. 5e which showed that all the materials exhibited decreased capacitive properties at higher scan rates. This is influenced by the pore structure in the material which is not fully accessible at an increased flow rate [73]. The dominant microporous character of carbon obtained

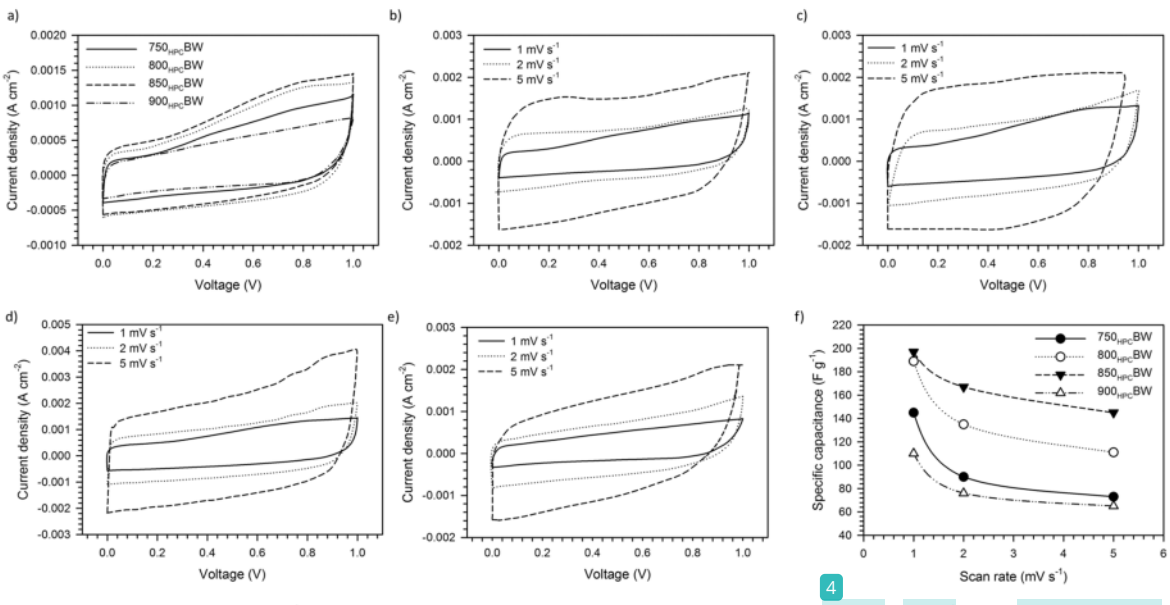

Fig. 5. (a) CV curve of $x_{HPC}BW$ in 1 mV s^{-1}, (b-e) CV curve of $750_{HPC}BW$, $800_{HPC}BW$, $850_{HPC}BW$ and $900_{HPC}BW$ in 1, 2, and 5 mV s^{-1}, and (f) specific capacitance vs. scan rate curve of $x_{HPC}BW$.

can significantly increase the charge storage capacity in the device, but due to their narrow pores, the electrolyte ion transport pathway is relatively disturbed at higher scanning rates. However, the 850_{HPC}BW displayed a relatively high-rate capability estimated to be 73% and this confirms its high potential as a sustainable electrode material that can be applied to high-performance devices.

An in-depth analysis to evaluate the capacitive properties of the 850_{HPC}BW electrode was comprehensively reviewed through the adoption of a galvanostatic charge-discharge approach at 1 A g^{-1} with a symmetric supercapacitor system. The GCD curves showing a symmetrical triangular shape with a slightly decreasing IR drop are presented in Fig. 6a and the characteristic profile suggests a normal-type double-layer capacitor with low internal resistance. This is in agreement with CV measurements which also confirmed a similar type of electrochemical behavior. Furthermore, the curved profile detected in the charging process was observed to be closely related to the degradation of the electrolyte ion due to the redox reaction of self-doping heteroatoms as confirmed by the CV measurements. The oxygen-nitrogen functional group was also found to be a dual self-doping heteroatom and this proves the presence of pseudo-capacitance in the carbon material prepared. It was discovered that the length of the x-axis with charge-discharge time variable reflects the capacitive properties of the electrode material and the 850_{HPC}BW material was observed to have displayed the longest charge-discharge curve, thereby, indicating the highest capacitive properties followed by 700_{HPC}BW, 750_{HPC}BW, and 900_{HPC}BW. Moreover, the measurement of the GCD showed that the specific capacitance of the electrodes 750_{HPC}BW, 800_{HPC}BW, 850_{HPC}BW, and 900_{HPC}BW was 123, 194, 202, and 98 F g^{-1} respectively. This shows an increase in the heat treatment in the CO_2 gas environment from 750 °C to 850 °C significantly increased the capacitive geometric properties of the electrodes by up to 57% due to the change in their morphological structure and porosity. The difference in pyrolysis temperature also significantly optimized the pore potential of the bread waste precursors such that their morphology at 850 °C confirmed a 3D hierarchical pore structure consisting of a combination of macropores, mesopores, and micropores with a specific surface area of 610.50 m^2 g^{-1}. Furthermore, the dominance of the micropores at 76.98% and the presence of mesopores at approximately 23.02% allow the electrode material to have abundant ion sites corresponding to the size of the electrolytic ions. This initiated several electric double layers and provided fast ion transfer pathways which increased the accessibility of charge flow in energy storage devices [74]. The combination of the optimized material properties also allowed the 850_{HPC}BW to have the highest capacitive properties but the excessive increase in temperature tended to damage the porosity features which subsequently led to a reduction in the specific capacitance as observed in the 900_{HPC}BW electrode. An in-depth analysis of the potential application of energy storage devices from a hierarchical porous carbon source based on bread waste was also reviewed through a Ragone plot as shown in Fig. 6b. It was generally discovered that the energy densities have an ideal range of values for supercapacitor applications and 850_{HPC}BW was found to have the most outstanding performance with the highest increased energy density of 11.61 Wh kg^{-1} at a power density of 156.71 W kg^{-1}. Moreover, the energy density obtained in the two-electrode configuration system was relatively high compared to those reported in previous studies as summarized in Table 3.

The behavior of ionic kinetics and further electrochemical verification of the hierarchical porous carbon based on breadcrumbs were confirmed using EIS measurements from low frequency (10mHz) to high frequency (100 kHz) at a constant amplitude of 10 mV. The focus was on the 750_{HPC}BW and 850_{HPC}BW samples observed to have experienced significant changes in their material and electrochemical properties due to quite different heat treatments. The Nyquist plot obtained is presented in Fig. 7a with two significantly different sections which generally indicate the ideal capacitive properties of EDLCs. The first part showed a semicircular pattern at high frequency which reflects the conductivity of the material for the diffusion of electrolyte ions [75]. The x-axis intersection in the region revealed the ohmic series equivalent resistance (R_s) which represents the intrinsic resistance of the electrolyte, the electrode-electrolyte contact resistance, the current-electrode-collector resistance, and the conductivity of the electrode material. It was discovered that 750_{HPC}BW exhibited low ohmic resistance of 0.16 Ω and an increase in the heat treatment from 750 °C to 850 °C led to a lower ohmic resistance value of 0.11 at 850_{HPC}BW. This means that 850 °C has a suitable pore structure with the aqueous electrolyte H_2SO_4 and the self-doping heteroatoms also maintain high conductivity. The second part showed nearly vertical curves which indicate the existence of normal capacitive properties in supercapacitor devices. The combination of these two patterns clearly showed that increasing the heat treatment from 750 °C to 850 °C can produce organic waste-based carbon electrode materials with high conductivity, low resistivity, and excellent capacitive properties leading to high performance in electrochemical energy storage devices. Furthermore, Fig. 7b shows the Bode phase plots of the 750_{HPC}BW and 850_{HPC}BW which represents the response of the carbonaceous materials to the H_2SO_4 electrolyte. It was discovered that the 850_{HPC}BW has a larger phase angle estimated at − 67° at low frequencies compared to − 54° recorded for 750_{HPC}BW and this confirms an increase in the fast response in line with the increment in the heat treatment, thereby, characterizing the improvement of the ideal capacitor as an electrode material [76]. The frequency and time responses of the 750_{HPC}BW and 850_{HPC}BW electrodes were also confirmed from the real capacitance and imaginary capacitance (C′-C″) sections with respect to frequency as presented in Fig. 7c and d. Moreover, a typical C′ versus frequency plot shows a high

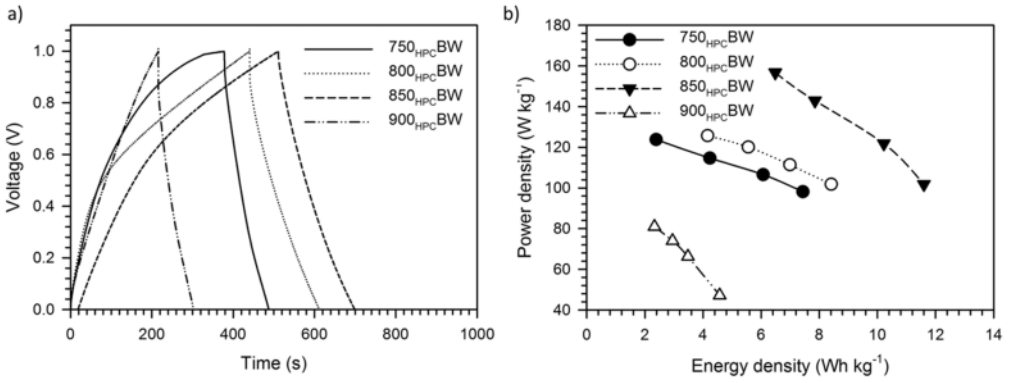

Fig. 6. (a) GCD curve of x_{HPC}BW, and (b) Ragone plot of x_{HPC}BW.

Table 3
The comparison of electrochemical properties of xHPCBW with other precursor in symmetrical supercapacitor tested.

Precursor	Morphology	S_{BET} ($m^2 g^{-1}$)	Electrolyte	C_{sp} ($F g^{-1}$)	E_{sp} ($Wh kg^{-1}$)	Ref.
Quinone-amine polymer	Nanospheres	2660	KOH	72.5	6.5	[77]
Oil palm stick	Hierarchical porous	631.262	H_2SO_4	256	21.19	[78]
Corncob	-		KOH	-	8.9	[44]
Watermelon peel	Sponge-like porous	1660	H_2SO_4	171	25.4	[79]
native European deciduous trees	-	614	H_2SO_4	24	0.53	[80]
Bread waste	Hierarchical porous	610.507	H_2SO_4	202	11.61	This work

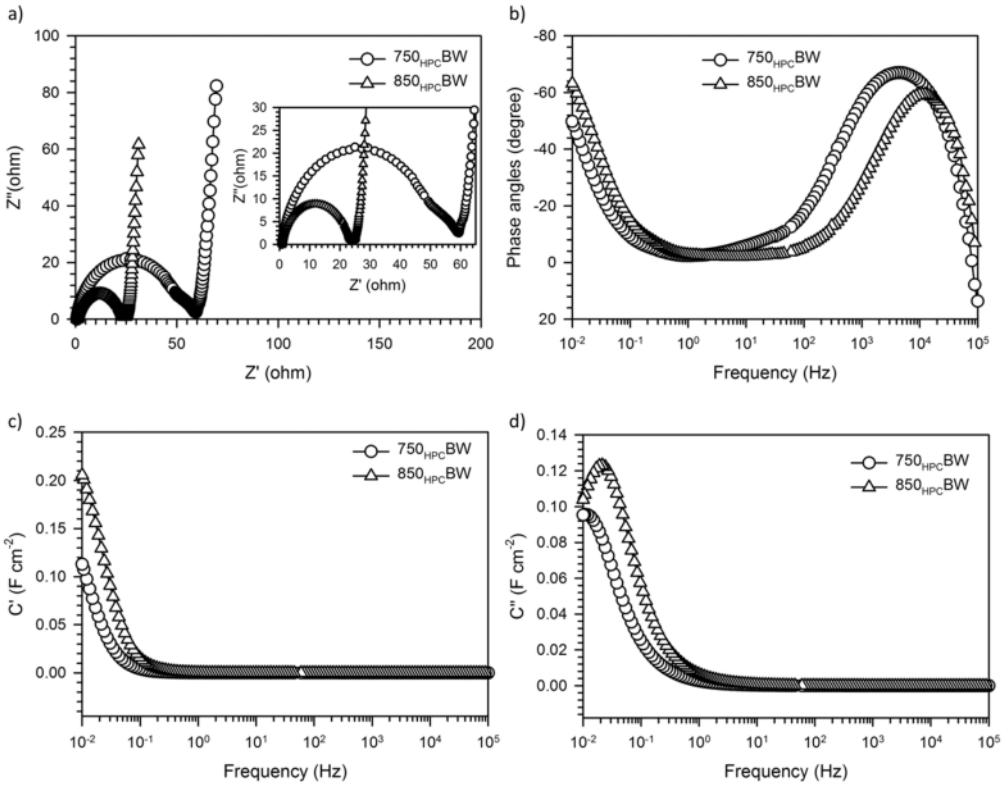

Fig. 7. (a) Nyquist plot, (b) Bode phase plot, (c) Bode plot in real capacitance, and (d) Bode plot in imaginer capacitance of $x_{HPC}BW$.

C′ response in the low-frequency region which indicates an ideal capacitive behavior and a very low C′ response at high frequency to confirm the inherited resistive features. The C'' vs. frequency plot further confirms the peak operating frequency of 0.014 Hz and 0.023 Hz with a low relaxation time constant that initiated the normal ion diffusion rate in carbon materials for supercapacitor applications.

4. Conclusion

In summary, 3D hierarchical porous activated carbon with dual self-doping heteroatoms was produced from a sustainable source of bread waste through a one-step physical activation strategy for subsequent application in high-performance supercapacitors. The dry bread wastes were physically activated in a CO_2 gas environment at stratified temperatures of 750, 800, 850, and 900 °C. This study did not involve any chemical impregnation to ensure the proposed approach was relatively time, cost, and labor efficient. The drastic increase in physical activation temperature was observed to have led to an optimized pore structure which is beneficial to the micro-mesopores combination. Moreover, the highest surface area of the carbon obtained was 610.50 $m^2 g^{-1}$ at a total volume of 0.391 $cm^3 g^{-1}$ with well-defined 3D hierarchical pores structures. The electrochemical properties were also measured on a coin solid design without the addition of a binder and the results showed a high specific capacitance of 202 $F g^{-1}$ at 1 $A g^{-1}$ in a 1 M H_2SO_4 electrolyte. Furthermore, the maximum energy density found in carbon synthesized at 850 °C was 11.61 $Wh kg^{-1}$ at a power density of 156.71 $W kg^{-1}$ with a low ohmic resistance of 0.11 Ω. This means the application of a one-step activation strategy for the synthesis of bread waste-derived 3D hierarchical porous activated carbon is an effective approach to producing high-performance supercapacitors.

CRediT authorship contribution statement

Rika Taslim: Conceptualization, Methodology. **Refky Refanza:** Resources, Writing – original draft. **Muhammad Ihsan Hamdy:** Visualization, Data curation. **Apriwandi Apriwandi:** Formal analysis, Writing – original draft, Writing – review & editing. **Erman Taer:** Methodology, Validation.

Declaration of Competing Interest

The authors declare the following financial interests/personal relationships which may be considered as potential competing interests: Rika Taslim reports was provided by State Islamic University Sultan Syarif Kasim Faculty of Science and Technology. Rika Taslim reports a relationship with State Islamic University Sultan Syarif Kasim Faculty of Science and Technology that includes: employment. Rika Taslim has patent pending to.

Data availability

Data will be made available on request.

Acknowledgments

The research was financially supported by collaborative grants between universities, State Islamic University of Sultan Syarif Kasim Riau with contract No. 873/Un.04/L.1/TL.01/03/2022. Also, second years Project of Word Class Research (WCR) in *Kementerian Pendidikan, Kebudayaan, Riset, dan Teknologi*, Republic of Indonesia.

References

[1] D.C. Wilson, L. Rodic, P. Modak, R. Soos, A.C. Rogero, C. Velis, M. Iyer, O. Simonett, Global Waste Management Outlook, 2016. ⟨https://doi.org/10.18356/765baec0-en⟩.
[2] B. Weber, Global recycling, Mag. Bus. Oppor. Int. Mark. 24 (2022) 1–48.
[3] C.P. Baldé, E. D'Angelo, V. Luda, O. Deubzer, R. Kuehr, Global Transboundary E-waste Flows Monitor 2022, 2022.
[4] OPMCSA, Food Waste A Global and Local Problem, 2022. ⟨https://www.pmcsa.ac.nz/files/2022/07/Food-Waste-A-global-and-local-problemv2.pdf⟩.
[5] P. Tamasiga, T. Miri, H. Onyeaka, A. Hart, Food waste and circular economy: challenges and opportunities, Sustainability 14 (2022), https://doi.org/10.3390/su14169896.
[6] R.K. Mishra, S.K. Ha, K. Verma, S.K. Tiwari, Recent progress in selected bio-nanomaterials and their engineering applications: an overview, J. Sci. Adv. Mater. Devices 3 (2018) 263–288, https://doi.org/10.1016/j.jsamd.2018.05.003.
[7] M. Şirazi, S. Aslan, Comprehensive characterization of high surface area activated carbon prepared from olive pomace by KOH activation, Chem. Eng. Commun. 0 (2021) 1–15, https://doi.org/10.1080/00986445.2020.1864628.
[8] A. Tursi, A review on biomass: importance, chemistry, classification, and conversion, Biofuel Res. J. 6 (2019) 962–979, https://doi.org/10.18331/BRJ2019.6.2.3.
[9] R.H. Bello, P. Linzmeyer, C.M.B. Franco, O. Souza, N. Sellin, S.H.W. Medeiros, C. Marangoni, Pervaporation of ethanol produced from banana waste, Waste Manag 34 (2014) 1501–1509, https://doi.org/10.1016/j.wasman.2014.04.013.
[10] S. Soltani, N. Khanian, T.S.Y. Choong, U. Rashid, Recent progress in the design and synthesis of nanofibers with diverse synthetic methodologies: Characterization and potential applications, New J. Chem. 44 (2020) 9581–9606, https://doi.org/10.1039/d0nj01071e.
[11] M. Changmai, P. Banerjee, K. Nahar, M.K. Purkait, A novel adsorbent from carrot, tomato and polyethylene terephthalate waste as a potential adsorbent for Co (II) from aqueous solution: kinetic and equilibrium studies, J. Environ. Chem. Eng. 6 (2018) 246–257, https://doi.org/10.1016/j.jece.2017.12.009.
[12] N. Bilandzija, N. Voca, B. Jelcic, V. Jurisic, A. Matin, M. Grubor, T. Kricka, Evaluation of croatian agricultural solid biomass energy potential, Renew. Sustain. Energy Rev. 93 (2018) 225–230, https://doi.org/10.1016/j.rser.2018.05.040.
[13] H. Yang, S. Ye, J. Zhou, T. Liang, Biomass-derived porous carbon materials for supercapacitor, Front. Chem. 7 (2019) 1–17, https://doi.org/10.3389/fchem.2019.00274.
[14] K. Aruchamy, K. Dharmalingam, C.W. Lee, D. Mondal, N. Sanna Kotrappanavar, Creating ultrahigh surface area functional carbon from biomass for high performance supercapacitor and facile removal of emerging pollutants, Chem. Eng. J. 427 (2022), 131477, https://doi.org/10.1016/j.cej.2021.131477.
[15] S.S. Sekhon, J.S. Park, Biomass-derived N-doped porous carbon nanosheets for energy technologies, Chem. Eng. J. 425 (2021), 129017, https://doi.org/10.1016/j.cej.2021.129017.
[16] N. Abuelnoor, A. AlHajaj, M. Khaleel, L.F. Vega, M.R.M. Abu-Zahra, Activated carbons from biomass-based sources for CO_2 capture applications, Chemosphere 282 (2021), 131111, https://doi.org/10.1016/j.chemosphere.2021.131111.
[17] X. Li, J. Zhang, B. Liu, Z. Su, A critical review on the application and recent developments of post-modified biochar in supercapacitors, J. Clean. Prod. 310 (2021), 127428, https://doi.org/10.1016/j.jclepro.2021.127428.
[18] W. Zhang, R.R. Cheng, H.H. Bi, Y.H. Lu, L.B. Ma, X.J. He, A review of porous carbons produced by template methods for supercapacitor applications, Xinxing Tan. Cailiao/New Carbon Mater. 36 (2021) 69–81, https://doi.org/10.1016/S1872-5805(21)60005-7.
[19] Y. Zhang, C. Wu, S. Dai, L. Liu, H. Zhang, W. Shen, W. Sun, C. Ming Li, Rationally tuning ratio of micro- to meso-pores of biomass-derived ultrathin carbon sheets toward supercapacitors with high energy and high power density, J. Colloid Interface Sci. 606 (2022) 817–825, https://doi.org/10.1016/j.jcis.2021.08.042.
[20] W. Li, C. Chen, H. Wang, P. Li, X. Jiang, J. Yang, J. Liu, Hierarchical porous carbon induced by inherent structure of eggplant as sustainable electrode material for high performance supercapacitor, J. Mater. Res. Technol. 17 (2022) 1540–1552, https://doi.org/10.1016/j.jmrt.2022.01.056.
[21] A. Jain, C. Xu, S. Jayaraman, R. Balasubramanian, J.Y. Lee, M.P. Srinivasan, Mesoporous activated carbons with enhanced porosity by optimal hydrothermal pre-treatment of biomass for supercapacitor applications, Microporous Mesoporous Mater. 218 (2015) 55–61, https://doi.org/10.1016/j.micromeso.2015.06.041.
[22] M. Shoaib, H.M. Al-Swaidan, Optimization and characterization of sliced activated carbon prepared from date palm tree fronds by physical activation, Biomass Bioenergy 73 (2015) 124–134, https://doi.org/10.1016/j.biombioe.2014.12.016.
[23] D. Bhattacharjya, J.S. Yu, Activated carbon made from cow dung as electrode material for electrochemical double layer capacitor, J. Power Sources 262 (2014) 224–231, https://doi.org/10.1016/j.jpowsour.2014.03.143.
[24] C.S. Yang, Y.S. Jang, H.K. Jeong, Bamboo-based activated carbon for supercapacitor applications, Curr. Appl. Phys. 14 (2014) 1616–1620, https://doi.org/10.1016/j.cap.2014.09.021.
[25] K. Wang, N. Zhao, S. Lei, R. Yan, X. Tian, J. Wang, Y. Song, D. Xu, Q. Guo, L. Liu, Promising biomass-based activated carbons derived from willow catkins for high performance supercapacitors, Electrochim. Acta 166 (2015) 1–11, https://doi.org/10.1016/j.electacta.2015.03.048.
[26] X. Chen, K. Wu, B. Gao, Q. Xiao, J. Kong, Q. Xiong, X. Peng, X. Zhang, J. Fu, Three-dimensional activated carbon recycled from rotten potatoes for high-performance supercapacitors, Waste Biomass Valoriz. 7 (2016) 551–557, https://doi.org/10.1007/s12649-015-9458-0.
[27] Y. Zhang, S. Yu, G. Lou, Y. Shen, H. Chen, Z. Shen, S. Zhao, J. Zhang, S. Chai, Q. Zou, Review of macroporous materials as electrochemical supercapacitor electrodes, J. Mater. Sci. 52 (2017) 11201–11228, https://doi.org/10.1007/s10853-017-0955-3.
[28] Y. Ma, X. Zhang, Z. Liang, C. Wang, Y. Sui, B/P/N/O co-doped hierarchical porous carbon nanofiber self-standing film with high volumetric and gravimetric capacitance performances for aqueous supercapacitors, Electrochim. Acta 337 (2020), 135800, https://doi.org/10.1016/j.electacta.2020.135800.
[29] E. Taer, A. Apriwandi, M.A. Mardiah, A. Awitdrus, R. Taslim, Synthesis free-template highly micro-mesoporous carbon nanosheet as electrode materials for boosting supercapacitor performances, Int. J. Energy Res. 46 (2022) 18740–18756, https://doi.org/10.1002/er.8493.
[30] X. Jiang, F. Guo, X. Jia, Y. Zhan, H. Zhou, L. Qian, Synthesis of nitrogen-doped hierarchical porous carbons from peanut shell as a promising electrode material for high-performance supercapacitors, J. Energy Storage 30 (2020), 101451, https://doi.org/10.1016/j.est.2020.101451.
[31] A.R. Selvaraj, A. Muthusamy, In-ho-Cho, H.J. Kim, K. Senthil, K. Prabakar, Ultrahigh surface area biomass derived 3D hierarchical porous carbon nanosheet electrodes for high energy density supercapacitors, Carbon 174 (2021) 463–474, https://doi.org/10.1016/j.carbon.2020.12.052.
[32] W. Duan, C. Fernández-Sánchez, M. Gich, Upcycling bread waste into a Ag-doped carbon material applied to the detection of halogenated compounds in waters, ACS Appl. Mater. Interfaces 14 (2022) 40182–40190, https://doi.org/10.1021/acsami.2c08332.
[33] V. Narisetty, R. Cox, N. Willoughby, E. Aktas, B. Tiwari, A.S. Matharu, K. Salonitis, V. Kumar, Recycling bread waste into chemical building blocks using a circular biorefining approach, Sustain. Energy Fuels 5 (2021) 4842–4849, https://doi.org/10.1039/d1se00575h.
[34] P. Konnerth, D. Jung, J.W. Straten, K. Raffelt, A. Kruse, Metal oxide-doped activated carbons from bakery waste and coffee grounds for application in supercapacitors, Mater. Sci. Energy Technol. 4 (2021) 69–80, https://doi.org/10.1016/j.mset.2020.12.008.
[35] E. Taer, M. Deraman, R. Taslim, Iwantono, Preparation of binderless activated carbon monolith from pre-carbonization rubber wood sawdust by controlling of carbonization and activation condition, AIP Conf. Proc. 1554 (2013) 33–37, https://doi.org/10.1063/1.4820277.
[36] A. Apriwandi, E. Taer, R. Farma, R.N. Setiadi, E. Amiruddin, A facile approach of micro-mesopores structure binder-free coin/monolith solid design activated carbon for electrode supercapacitor, J. Energy Storage 40 (2021), 102823, https://doi.org/10.1016/j.est.2021.102823.
[37] E. Taer, A. Apriwandi, D. Rama, Solid coin-like design activated carbon nanospheres derived from shallot peel precursor for boosting supercapacitor performance, J. Mater. Res. Technol. 15 (2021) 1732–1741, https://doi.org/10.1016/j.jmrt.2021.09.025.
[38] E. Taer, K. Natalia, A. Apriwandi, R. Taslim, A. Agustino, R. Farma, The synthesis of activated carbon nano fiber electrode made from acacia leaves (Acacia mangium wild) as supercapacitors, Adv. Nat. Sci. Nanosci. Nanotechnol. 11 (2020) 25007, https://doi.org/10.1088/2043-6254/ab8b60.
[39] A. Yaya, B. Agyei-Tuffour, D. Dodoo-Arhin, E. Nyankson, E. Annan, D.S. Konadu, E. Sinayobye, E.A. Baryeh, C.P. Ewels, Layered nanomaterials-a review, Glob. J. Eng. Des. Technol. 1 (2012) 32–41. ⟨http://www.gifre.org/admin/papers/gjedt/1222-32-41.pdf⟩.
[40] D. Dahlan, N. Sartika, Astuti, E.L. Namigo, E. Taer, Effect of TiO2 on duck eggshell membrane as separators in supercapacitor applications, Mater. Sci. Forum 827 (2015) 151–155, https://doi.org/10.4028/www.scientific.net/MSF.827.151.
[41] E. Taer, Y. Susanti, A. Awitdrus, S. Sugianto, R. Taslim, R.N. Setiadi, S. Bahri, A. Agustino, P. Dewi, B. Kurniasih, The effect of CO_2 activation temperature on the

physical and electrochemical properties of activated carbon monolith from banana stem waste, 030016–1–030016–5, AIP Conf. Proc. 1927 (2018), https://doi.org/10.1063/1.5021209.
[42] P. Kalyani, A. Anitha, Biomass carbon & its prospects in electrochemical energy systems, Int. J. Hydrog. Energy 38 (2013) 4034–4045, https://doi.org/10.1016/j.ijhydene.2013.01.048.
[43] L. Suárez, T.A. Centeno, Unravelling the volumetric performance of activated carbons from biomass wastes in supercapacitors, J. Power Sources 448 (2020), 227413, https://doi.org/10.1016/j.jpowsour.2019.227413.
[44] M. Xu, Q. Huang, J. Lu, J. Niu, Green synthesis of high-performance supercapacitor electrode materials from agricultural corncob waste by mild potassium hydroxide soaking and a one-step carbonization, Ind. Crop. Prod. 161 (2021), 113215, https://doi.org/10.1016/j.indcrop.2020.113215.
[45] Y. Liu, Z. Chang, L. Yao, S. Yan, J. Lin, J. Chen, J. Lian, H. Lin, S. Han, Nitrogen/sulfur dual-doped sponge-like porous carbon materials derived from pomelo peel synthesized at comparatively low temperatures for superior-performance supercapacitors, J. Electroanal. Chem. 847 (2019), 113111, https://doi.org/10.1016/j.jelechem.2019.04.071.
[46] Y. Wang, M. Qiao, X. Mamat, Nitrogen-doped macro-meso-micro hierarchical ordered porous carbon derived from ZIF-8 for boosting supercapacitor performance, Appl. Surf. Sci. 540 (2021), 148352, https://doi.org/10.1016/j.apsusc.2020.148352.
[47] M. Wu, S. Xu, X. Li, T. Zhang, Z. Lv, Z. Li, X. Li, Pore regulation of wood-derived hierarchical porous carbon for improving electrochemical performance, J. Energy Storage 40 (2021), 102663, https://doi.org/10.1016/j.est.2021.102663.
[48] N. Sangtong, T. Chaisuwan, S. Wongkasemjit, H. Ishida, W. Redpradit, K. Seneesrisakul, U. Thubsuang, Ultrahigh-surface-area activated biocarbon based on biomass residue as a supercapacitor electrode material: tuning pore structure using alkalis with different atom sizes, Microporous Mesoporous Mater. 326 (2021), 111383, https://doi.org/10.1016/j.micromeso.2021.111383.
[49] T. Chen, L. Luo, L. Luo, J. Deng, X. Wu, M. Fan, G. Du, Weigang Zhao, High energy density supercapacitors with hierarchical nitrogen-doped porous carbon as active material obtained from bio-waste, Renew. Energy 175 (2021) 760–769, https://doi.org/10.1016/j.renene.2021.05.006.
[50] M.D. Liao, C. Peng, S.P. Hou, J. Chen, X.G. Zeng, H.L. Wang, J.H. Lin, Large-scale synthesis of nitrogen-doped activated carbon fibers with high specific surface area for high-performance supercapacitors, Energy Technol. 8 (2020) 1901477, https://doi.org/10.1002/ente.201901477.
[51] L.K.C. de Souza, A.A.S. Gonçalves, L.S. Queiroz, J.S. Chaar, G.N. da Rocha Filho, C. E.F. da Costa, Utilization of acai stone biomass for the sustainable production of nanoporous carbon for CO_2 capture, Sustain. Mater. Technol. 25 (2020), e00168, https://doi.org/10.1016/j.susmat.2020.e00168.
[52] E. Taer, A. Afrianda, R. Taslim, Krisman Minarni, A. Agustino, A. Apriwandi, U. Malik, The physical and electrochemical properties of activated carbon electrode made from Terminalia catappa leaf (TCL) for supercapacitor cell application, J. Phys. Conf. Ser. 1120 (2018), 012007, https://doi.org/10.1088/1742-6596/1120/1/012007.
[53] F. Márquez-Montesino, N. Torres-Figueredo, A. Lemus-Santana, F. Trejo, Activated carbon by potassium carbonate activation from pine sawdust (Pinus montezumae Lamb.), Chem. Eng. Technol. 43 (2020) 1716–1725, https://doi.org/10.1002/ceat.202000051.
[54] E. Taer, R. Taslim, A. Apriwandi, Ultrahigh capacitive supercapacitor derived from self-oxygen doped biomass-based 3D porous carbon sources, ChemNanoMat 8 (2022), e202100388, https://doi.org/10.1002/cnma.202100388.
[55] A.M. Abioye, F.N. Ani, Recent development in the production of activated carbon electrodes from agricultural waste biomass for supercapacitors: a review, Renew. Sustain. Energy Rev. 52 (2015) 1282–1293, https://doi.org/10.1016/j.rser.2015.07.129.
[56] F. Liu, Z. Wang, H. Zhang, L. Jin, X. Chu, B. Gu, H. Huang, W. Yang, Nitrogen, oxygen and sulfur co-doped hierarchical porous carbons toward high-performance supercapacitors by direct pyrolysis of kraft lignin, Carbon 149 (2019) 105–116, https://doi.org/10.1016/j.carbon.2019.04.023.
[57] J. Serafin, M. Baca, M. Biegun, E. Mijowska, R.J. Kaleńczuk, J. Sreńscek-Nazzal, B. Michalkiewicz, Direct conversion of biomass to nanoporous activated biocarbons for high CO_2 adsorption and supercapacitor applications, Appl. Surf. Sci. 497 (2019), 143722, https://doi.org/10.1016/j.apsusc.2019.143722.
[58] K. Kumar, R.K. Saxena, R. Kothari, D.K. Suri, N.K. Kaushik, J.N. Bohra, Correlation between adsorption and x-ray diffraction studies on viscose rayon based activated carbon cloth, Carbon 35 (1997) 1842–1844, https://doi.org/10.1016/S0008-6223(97)87258-2.
[59] M. Deraman, R. Daik, S. Soltaninejad, N.S.M. Nor, Awitdrus, R. Farma, N. F. Mamat, N.H. Basri, M.A.R. Othman, A new empirical equation for estimating specific surface area of supercapacitor carbon electrode from X-ray diffraction, Adv. Mater. Res. 1108 (2015) 1–7, https://doi.org/10.4028/www.scientific.net/AMR.1108.1.
[60] A. Sarwar, M. Ali, A.H. Khoja, A. Nawar, A. Waqas, R. Liaquat, S.R. Naqvi, M. Asjid, Synthesis and characterization of biomass-derived surface-modified activated carbon for enhanced CO_2 adsorption, J. CO_2 Util. 46 (2021), 101476, https://doi.org/10.1016/j.jcou.2021.101476.
[61] E. Taer, A. Agustino, A. Awitdrus, R. Farma, R. Taslim, The synthesis of carbon nanofiber derived from pineapple leaf fibers as a carbon electrode for supercapacitor application, J. Electrochem. Energy Convers. Storage 18 (2020) 1–24, https://doi.org/10.1115/1.4048405.
[62] R.T. Ayinla, J.O. Dennis, H.M. Zaid, Y.K. Sanusi, F. Usman, L.L. Adebayo, A review of technical advances of recent palm bio-waste conversion to activated carbon for energy storage, J. Clean. Prod. 229 (2019) 1427–1442, https://doi.org/10.1016/j.jclepro.2019.04.116.
[63] L. Luo, Y. Zhou, W. Yan, X. Wu, S. Wang, W. Zhao, Two-step synthesis of B and N co-doped porous carbon composites by microwave-assisted hydrothermal and pyrolysis process for supercapacitor application, Electrochim. Acta 360 (2020), https://doi.org/10.1016/j.electacta.2020.137010.
[64] M.Z. Iqbal, S. Zakar, S.S. Haider, Role of aqueous electrolytes on the performance of electrochemical energy storage device, J. Electroanal. Chem. 858 (2020), 113793, https://doi.org/10.1016/j.jelechem.2019.113793.
[65] J. Du, H. Lv, Y. Yu, A. Chen, Construction of dual-mesoporous carbon fibers via coassembly for supercapacitors, Phys. Status Solidi Appl. Mater. Sci. 217 (2020) 1–6, https://doi.org/10.1002/pssa.202000365.
[66] G.A. Yakaboylu, C. Jiang, T. Yumak, J.W. Zondlo, J. Wang, E.M. Sabolsky, Engineered hierarchical porous carbons for supercapacitor applications through chemical pretreatment and activation of biomass precursors, Renew. Energy 163 (2021) 276–287, https://doi.org/10.1016/j.renene.2020.08.092.
[67] S. Majid, A.S.G. Ali, W.Q. Cao, R. Reza, Q. Ge, Biomass-derived porous carbons as supercapacitor electrodes-a review, New Carbon Mater. 36 (2021) 546–572, https://doi.org/10.1016/S1872-5805(21)60038-0.
[68] Y. Guo, T. Wang, D. Wu, Y. Tan, One-step synthesis of in-situ N, S self-doped carbon nanosheets with hierarchical porous structure for high performance supercapacitor and oxygen reduction reaction electrocatalyst, Electrochim. Acta 366 (2021), 137404, https://doi.org/10.1016/j.electacta.2020.137404.
[69] A. Gopalakrishnan, S. Badhulika, Effect of self-doped heteroatoms on the performance of biomass-derived carbon for supercapacitor applications, J. Power Sources 480 (2020), 228830, https://doi.org/10.1016/j.jpowsour.2020.228830.
[70] H. Yang, J. Zhou, M. Wang, S. Wu, W. Yang, H. Wang, From basil seed to flexible supercapacitors: green synthesis of heteroatom-enriched porous carbon by self-gelation strategy, Int. J. Energy Res. 44 (2020) 4449–4463, https://doi.org/10.1002/er.5222.
[71] F. Ran, X. Yang, X. Xu, S. Li, Y. Liu, L. Shao, Green activation of sustainable resources to synthesize nitrogen-doped oxygen-riched porous carbon nanosheets towards high-performance supercapacitor, Chem. Eng. J. 412 (2021), 128673, https://doi.org/10.1016/j.cej.2021.128673.
[72] X. Hao, J. Wang, B. Ding, Y. Wang, Z. Chang, H. Dou, X. Zhang, Bacterial-cellulose-derived interconnected meso-microporous carbon nanofiber networks as binder-free electrodes for high-performance supercapacitors, J. Power Sources 352 (2017) 34–41, https://doi.org/10.1016/j.jpowsour.2017.03.088.
[73] Y. Wang, Z. Zhao, W. Song, Z. Wang, X. Wu, From biological waste to honeycomb-like porous carbon for high energy density supercapacitor, J. Mater. Sci. 54 (2019) 4917–4927, https://doi.org/10.1007/s10853-018-03215-8.
[74] D. Chinnadurai, H.J. Kim, S. Karupannan, K. Prabakar, Multiscale honeycomb-structured activated carbon obtained from nitrogen-containing mandarin peel: high-performance supercapacitors with significant cycling stability, New J. Chem. 43 (2019) 3486–3492, https://doi.org/10.1039/C8NJ05895D.
[75] Atika, R.K. Dutta, Oxygen-rich porous activated carbon from eucalyptus wood as an efficient supercapacitor electrode, Energy Technol. 9 (2021) 1–12, https://doi.org/10.1002/ente.202100463.
[76] C. Huettner, F. Xu, S. Paasch, C. Kensy, Y.X. Zhai, J. Yang, E. Brunner, S. Kaskel, Ultra-hydrophilic porous carbons and their supercapacitor performance using pure water as electrolyte, Carbon 178 (2021) 540–551, https://doi.org/10.1016/j.carbon.2021.03.013.
[77] Z. Song, D. Zhu, L. Li, T. Chen, H. Duan, Z. Wang, Y. Lv, W. Xiong, M. Liu, L. Gan, Ultrahigh energy density of a N, O codoped carbon nanosphere based all-solid-state symmetric supercapacitor, J. Mater. Chem. A 7 (2019) 1177–1186, https://doi.org/10.1039/c8ta10158b.
[78] Julnaidi, E. Saputra, Nofrizal, E. Taer, Renewable palm oil sticks biomass-derived unique hierarchical porous carbon nanostructure as sustainability electrode for symmetrical supercapacitor, J. Chem. Technol. Biotechnol. 98 (2023) 45–56, https://doi.org/10.1002/jctb.7217.
[79] P. Zhang, J. Mu, Z. Guo, S.I. Wong, J. Sunarso, Y. Zhao, W. Xing, J. Zhou, S. Zhuo, Watermelon peel-derived heteroatom-doped hierarchical porous carbon as a high-performance electrode material for supercapacitors, ChemElectroChem 8 (2021) 1196–1203, https://doi.org/10.1002/celc.202100267.
[80] A. Jain, M. Ghosh, M. Krajewski, S. Kurungot, M. Michalska, Biomass-derived activated carbon material from native European deciduous trees as an inexpensive and sustainable energy material for supercapacitor application, J. Energy Storage 34 (2021), 102178, https://doi.org/10.1016/j.est.2020.102178.

One-step strategy of 3D hierarchical porous carbon with self-heteroatom-doped derived bread waste for high-performance supercapacitor

ORIGINALITY REPORT

14%	7%	13%	5%
SIMILARITY INDEX	INTERNET SOURCES	PUBLICATIONS	STUDENT PAPERS

PRIMARY SOURCES

1	Guofeng Qiu, Zekai Miao, Yang Guo, Jie Xu, Wenke Jia, Yixin Zhang, Fanhui Guo, Jianjun Wu. "Bamboo-based hierarchical porous carbon for high-performance supercapacitors: the role of different components", Colloids and Surfaces A: Physicochemical and Engineering Aspects, 2022 Publication	1%
2	Submitted to Xiamen University Student Paper	1%
3	electrochemsci.org Internet Source	1%
4	Erman Taer, Muhammad Ali Akbar Tsalis, Apriwandi, Novi Yanti, Awitdrus, Lazuardi, Rika Taslim. "Porous Activated Carbon Binder-free Scleria sumatrensis Stem-Based for Supercapacitor Application", Journal of Physics: Conference Series, 2021 Publication	<1%

5	Erman Taer, Apriwandi Apriwandi, Widya Febriani, Rika Taslim. " Suitable Micro/Mesoporous Carbon Derived from Galangal Leaves (.) Biomass for Enhancing Symmetric Electrochemical Double - layer Capacitor Performances ", ChemistrySelect, 2022 Publication	<1 %
6	Erman Taer, Apriwandi Apriwandi, Agustino Agustino, Mega Ratna Dewi, Rika Taslim. "Porous hollow biomass - based carbon nanofiber/nanosheet for high - performance supercapacitor", International Journal of Energy Research, 2021 Publication	<1 %
7	E Taer, Nursyafni, Apriwandi, R Taslim. "High Potential of Averrhoa bilimbi Leaf Waste as Porous Activated Carbon Source for Sustainable Electrode Material Supercapacitor", Journal of Physics: Conference Series, 2021 Publication	<1 %
8	Jinhao Zhang, Hou Chen, Jiabao Bai, Ming Xu, Chenli Luo, Lixia Yang, Liangjiu Bai, Donglei Wei, Wenxiang Wang, Huawei Yang. "N-doped hierarchically porous carbon derived from grape marcs for high-performance	<1 %

supercapacitors", Journal of Alloys and Compounds, 2021
Publication

9	Submitted to University College London Student Paper	<1 %
10	Feitian Ran, Xiaobin Yang, Xueqing Xu, Songwei Li, Yuyan Liu, Lu Shao. "Green Activation of Sustainable Resources to Synthesize Nitrogen-doped Oxygen-riched Porous Carbon Nanosheets towards High-performance Supercapacitor", Chemical Engineering Journal, 2021 Publication	<1 %
11	Submitted to Universitas Riau Student Paper	<1 %
12	www.ippt.pan.pl Internet Source	<1 %
13	mafiadoc.com Internet Source	<1 %
14	Chenjun He, Mei Huang, Li Zhao, Yongjia Lei, Jinsong He, Dong Tian, Yongmei Zeng, Fei Shen, Jianmei Zou. "Enhanced electrochemical performance of porous carbon from wheat straw as remolded by hydrothermal processing", Science of The Total Environment, 2022 Publication	<1 %

15	aip.scitation.org Internet Source	<1%
16	Submitted to Indian Institute of Technology, Kanpur Student Paper	<1%
17	Erman Taer, Nazilah Nikmatun, Apriwandi, Agustino, Rika Taslim, Ezri Hidayat. "The Self-Adhesive Carbon Powder Based on Coconut Coir Fiber as Supercapacitor Application", Journal of Metastable and Nanocrystalline Materials, 2021 Publication	<1%
18	Milena Giulia Gonçalves. "História natural da infecção por variantes genéticas de HPV-16 no canal anal de homens participantes do estudo internacional multicêntrico HIM (HPV Infection in Men)", Universidade de Sao Paulo, Agencia USP de Gestao da Informacao Academica (AGUIA), 2022 Publication	<1%
19	air.repo.nii.ac.jp Internet Source	<1%
20	Xun Chen, Manzhou Chi, Linlin Xing, Xuan Xie et al. "Natural Plant Template-Derived Cellular Framework Porous Carbon as a High-Rate and Long-Life Electrode Material for Energy	<1%

Storage", ACS Sustainable Chemistry & Engineering, 2019
Publication

21	Jiahui Mu, Shao Ing Wong, Qiang Li, Pengfei Zhou, Jin Zhou, Yi Zhao, Jaka Sunarso, Shuping Zhuo. "Fishbone-derived N-doped hierarchical porous carbon as an electrode material for supercapacitor", Journal of Alloys and Compounds, 2020 Publication	<1 %
22	T. Arul Raja, Palanisamy Vickraman, A. Simon Justin, B. Joji Reddy. "Electrochemical studies on NH4MnPO4.H2O–rGO Hybrid Composite Synthesized via Microwave Route for High Energy Supercapacitors", Journal of Materials Science, 2020 Publication	<1 %
23	Submitted to University of Western Ontario Student Paper	<1 %
24	R. Ragavan, A. Pandurangan. "Exploration on magnetic and electrochemical properties of nitrogen and phosphorus Co-doped ordered mesoporous carbon for supercapacitor applications", Microporous and Mesoporous Materials, 2022 Publication	<1 %
25	M. Karnan, K. Subramani, N. Sudhan, N. Ilayaraja, M. Sathish. " Derived Activated High-	<1 %

Surface-Area Carbon for Flexible and High-Energy Supercapacitors ", ACS Applied Materials & Interfaces, 2016
Publication

26	real.mtak.hu Internet Source	<1 %
27	Dinda Pertiwi, Novi Yanti, Rika Taslim. "High potential of yellow potato (Solanum Tuberosum L.) peel waste as porous carbon source for supercapacitor electrodes", Journal of Physics: Conference Series, 2022 Publication	<1 %
28	Erman Taer, Friska Febriyanti, Widya Sinta Mustika, Rika Taslim, Agustino Agustino, Apriwandi Apriwandi. "Enhancing the performance of supercapacitor electrode from chemical activation of carbon nanofibers derived Areca catechu husk via one-stage integrated pyrolysis", Carbon Letters, 2020 Publication	<1 %
29	Submitted to University of Sheffield Student Paper	<1 %
30	Windasari, Rika Taslim. "Conversion of Salam leaves (Syzygium polyanthum (Wight) Walp.) bio-kitchen waste as functional activated carbon for sustainable supercapacitor electrodes", Journal of Physics: Conference Series, 2022	<1 %

Publication

31	Rakhmawati Farma, Arum Indriani, Irma Apriyani. "Hierarchical-nanofiber structure of biomass-derived carbon framework with direct CO2 activation for symmetrical supercapacitor electrodes", Journal of Materials Science: Materials in Electronics, 2023 Publication	<1 %
32	Deqian Meng, Chengfeng Wu, Yunzhi Hu, Yidan Jing, Xiaomin Zhang, Sakil Mahmud, Sheng Pei Su, Jin Zhu. "Ingenious synthesis of chitosan-based porous carbon supercapacitors with large specific area by a small amount of potassium hydroxide", Journal of Energy Storage, 2022 Publication	<1 %
33	Submitted to Indian Institute of Space Science and Technology Student Paper	<1 %
34	Alekha Tyagi, Prerna Sinha, Kamal K. Kar, Hiroyuki Yokoi. "Acid-directed preparation of micro/mesoporous heteroatom doped defective graphitic carbon as bifunctional electroactive material: Evaluation of trace metal impurity", Journal of Colloid and Interface Science, 2021 Publication	<1 %

35	Changshui Wang, Bing Yan, Jiaojiao Zheng, Li Feng et al. "Recent Progress in Template-Assisted Synthesis of Porous Carbons for Supercapacitors", Advanced Powder Materials, 2021 Publication	<1 %
36	rua.ua.es Internet Source	<1 %
37	Liu Wan, Dequan Chen, Jiaxing Liu, Yan Zhang, Jian Chen, Cheng Du, Mingjiang Xie. "Facile preparation of porous carbons derived from orange peel via basic copper carbonate activation for supercapacitors", Journal of Alloys and Compounds, 2020 Publication	<1 %
38	pub.iapchem.org Internet Source	<1 %
39	www.pnas.org Internet Source	<1 %
40	Aravindha Raja Selvaraj, Anand Muthusamy, Inho-Cho, Hee-Je Kim, Karuppanan Senthil, Kandasamy Prabakar. "Ultrahigh surface area biomass derived 3D hierarchical porous carbon nanosheet electrodes for high energy density supercapacitors", Carbon, 2021 Publication	<1 %

41 Bhaskar J. Choudhury, Harrison Hihu Muigai, Pankaj Kalita, Vijayanand S. Moholkar. "Biomass blend derived porous carbon for aqueous supercapacitors with commercial-level mass loadings and enhanced energy density in redox-active electrolyte", Applied Surface Science, 2022 <1%
Publication

42 Glaydson Simões dos Reis, Ravi Moreno A. Pinheiro Lima, Sylvia H. Larsson, Chandrasekar Mayandi Subramaniyam et al. "Flexible supercapacitors of biomass-based activated carbon-polypyrrole on eggshell membranes", Journal of Environmental Chemical Engineering, 2021 <1%
Publication

43 Huanxi Liao, Longsheng Zhong, Yatian Deng, Hongneng Chen, Guohua Liao, Yanhe Xiao, Baochang Cheng, Shuijin Lei. "A systematic study on Equisetum ramosissimum Desf. derived honeycomb porous carbon for supercapacitors: Insight into the preparation-structure-performance relationship", Applied Surface Science, 2023 <1%
Publication

44 Li-Feng Chen, Xu-Dong Zhang, Hai-Wei Liang, Mingguang Kong, Qing-Fang Guan, Ping Chen, Zhen-Yu Wu, Shu-Hong Yu. "Synthesis of <1%

Nitrogen-Doped Porous Carbon Nanofibers as an Efficient Electrode Material for Supercapacitors", ACS Nano, 2012
Publication

45	Mutian Ma, Weijie Cai, Yongli Chen, Yuan Li, Fengzhi Tan, Jinghui Zhou. "Flower-like NiMn-layered double hydroxide microspheres coated on biomass-derived 3D honeycomb porous carbon for high-energy hybrid supercapacitors", Industrial Crops and Products, 2021 Publication	<1 %
46	Nada Abuelnoor, Ahmed AlHajaj, Maryam Khaleel, Lourdes F. Vega, Mohammad R.M. Abu-Zahra. "Activated Carbons from Biomass-Based Sources for CO2 Capture Applications", Chemosphere, 2021 Publication	<1 %
47	profdoc.um.ac.ir Internet Source	<1 %
48	www.polymer.cn Internet Source	<1 %
49	www2.mdpi.com Internet Source	<1 %
50	Lulu Wang, Xuejian Li, Xing Huang, Sheng Han, Jibo Jiang. "Activated green resources to synthesize N, P co-doped O-rich hierarchical	<1 %

interconnected porous carbon for high-performance supercapacitors", Journal of Alloys and Compounds, 2022
Publication

---

51 Marta Sevilla, Antonio B. Fuertes. "Direct Synthesis of Highly Porous Interconnected Carbon Nanosheets and Their Application as High-Performance Supercapacitors", ACS Nano, 2014 <1%
Publication

---

52 Rakhmawati Farma, Mutya Kusumasari, Irma Apriyani, Awitdrus Awitdrus. "The production of carbon electrodes from lignocellulosic biomass of areca midrib through a chemical activation process for supercapacitor cells application", Energy Sources, Part A: Recovery, Utilization, and Environmental Effects, 2021 <1%
Publication

---

53 Xingtong Meng, Shuai Jia, Lanlan Mo, Jie Wei, Feijun Wang, Ziqiang Shao. "O/N-co-doped hierarchically porous carbon from carboxymethyl cellulose ammonium for high-performance supercapacitors", Journal of Materials Science, 2020 <1%
Publication

---

54 Yang, J.. "Carbon Electrode Material with High Densities of Energy and Power", Acta Physico- <1%

	Chimica Sinica, 200801 Publication	
55	expert.taylors.edu.my Internet Source	<1 %
56	lppm.unri.ac.id Internet Source	<1 %
57	mts.intechopen.com Internet Source	<1 %
58	pureadmin.qub.ac.uk Internet Source	<1 %
59	www.frontiersin.org Internet Source	<1 %
60	www.tandfonline.com Internet Source	<1 %
61	"Engineered Biochar", Springer Science and Business Media LLC, 2022 Publication	<1 %
62	Ming Zhang, Dingyu Yang, Jitao Li. "Ultrasonic and NH4+ assisted Ni foam substrate oxidation to achieve high performance MnO2 supercapacitor", Applied Surface Science, 2021 Publication	<1 %
63	Yuto Kurihara, Toru Takahashi, Rieko Osu. "The topology of interpersonal neural network	<1 %

in weak social ties", Cold Spring Harbor Laboratory, 2023
Publication

64 Diego Ramón Lobato-Peralta, Rayko Amaro, D.M. Arias, Ana Karina Cuentas-Gallegos et al. "Activated carbon from wasp hive for aqueous electrolyte supercapacitor application", Journal of Electroanalytical Chemistry, 2021 <1%
Publication

65 Mengge Shang, Jing Zhang, Xiaochan Liu, Yi Liu, Sipeng Guo, Shimo Yu, Serguei Filatov, Xibin Yi. "N, S self-doped hollow-sphere porous carbon derived from puffball spores for high performance supercapacitors", Applied Surface Science, 2021 <1%
Publication

Exclude quotes	On	Exclude matches	Off
Exclude bibliography	On		